THE EFFECT OF WATER ON METAKAOLIN PHOSPHATE-BASED GEOPOLYMER PROPERTIES

QINGBO TIAN*, XIN YU*, YUWU SUI*, # LINA XU*, ZHIJIE LV**

*School of Materials Science and Engineering, Shandong Jianzhu University, Jinan, China;
**School of Mechanical and Electrical Engineering, Shandong Jianzhu University, Jinan, China

#E-mail: Xu_ln2007@126.com

The work deals with the synthesis of metakaolin phosphate-based geopolymers (MKPGs) using calcined kaolin, phosphoric acid (PA), and mixing water. The metakaolin was thermally treated at 750 °C for different holding times. The different duration in the heating at 750 °C led to the gradual dehydroxylation of kaolin to metakaolin with a different structural water content (inter-layer and inner-layer residual water). Considering the temperature or duration of the thermal dehydroxylation, the inter-layer water evolved first, followed by the inner-layer water at a higher temperature or later time. The polymerisation degree is closely linked with the presence of the inter- or inner-layer water. It was found that the inter-layer residual water negatively influences the compressive strength, while the water in the inner-layer exerts a more negligible effect on the resistance. Indeed, the inter-layer water loss is linked to the structural changes in kaolinite; but the loss of water from the inner-layer is related to the structural changes in the metakaolinite. The holding time of dehydroxylation and water-to-metakaolin (W/M) ratio were optimised. A maximum strength of 57.6 MPa was achieved at the Al/P and W/M ratios of 1.0 and 0.40, respectively. The mass losses at the different temperatures showed that the additional excess mixing water increased the porosity of the MKPGs, resulting in a decrease in the compressive strength.

INTRODUCTION

Geopolymers are chains or networks of amorphous or semi-crystalline three-dimensional materials [1,2], obtained by aluminosilicate containing materials activated in an alkaline medium with sodium (potassium) hydroxide or sodium silicate [3] and in an acidic medium with phosphoric acid or humic acids [4-6]. Compared with alkaline-based geopolymers, phosphate-based materials are a new variety of geopolymers, but have attracted more interest due to their lower alkali ion leakage levels, higher strength and thermal stability, and lower dielectric constant [2,5,7-11].

Metakaolin (MK), which is transformed from kaolinite by the dehydroxylation reaction, is usually used as the raw material of acid-based geopolymers due to its high reactivity and simple chemical composition [12]. The characteristics of MK are crucial in the fabrication of metakaolin phosphate-based geopolymers (MKPGs) as MK supplies Al^{3+} to form the bond with phosphate groups. Generally, MK is formed between 400 °C and 700 °C by a gradual loss of structural water accompanied by the collapse of the interlayer space and the structural changes in the Al^{3+} coordination from six- to four-fold [13]. However, the degrees of dehydroxylation are different due to resources of kaolin and the calcining temperature [8, 14]. According to Cao *et al.* [15], 11.23 % inter-layer structural water and 3.65 % inner-layer water were dehydroxylated at about 200-430 °C and 520-800 °C, respectively. Gasparini *et al.* [14] found that only *ca*. 0.5 % adsorbed water was removed from kaolinite below 450 °C and kaolinite was not completely transformed to metakaolinite even after a long time at 450 °C. In the range of 450-800 °C, which varied somewhat depending on the resources of kaolin, kaolinite was transformed into amorphous metakaolinite and became more reactive.

The formation of MKPGs starts with the dissolution of MK into an acid leading to the release of Al^{3+} ions, which then polycondense with the phosphorous entities to form three-dimensional hydrated aluminophosphate networks [16]. During the dissolution of MK, it is essential to adjust the water to control the degree of polymerisation of the phosphoric acid, which will control the polycondensation reaction [17]. The amount of water affects the setting time and viscosity of the mixture, further influencing the structural phases and mechanical properties of MKGPs [18]. In addition, the residual water in the calcined kaolin is another factor influencing such geopolymeric processes. Cao *et al.* [15] found that either too much or too little residual water in the kaolin decreased the activity of the MK. The former was due to an uncomplete transformation to metakaolinite; while the latter was because the layer structures of the metakaolinite collapsed. However, Derouiche and Baklouti [19] prepared a compact MKGP

by mechanochemical activation of the kaolin, in which the MK is not rendered completely amorphous; they concluded that the complete dehydroxylation of kaolinite did not cause the lower activity of the MK. Based on the conclusion of Sperinck *et al.* [13], the kaolinite structure was completely lost at 80 % dehydroxylation, which meant that there were residual OH groups left in the metakaolinite structure before an anhydrous phase was completely formed [14]. Therefore, although the transformation processes of kaolin to MK have been well investigated, the influences of the degree of dehydroxylation and the structural changes of kaolin on the geopolymerisation are still unclear. In the present research, the effects of residual water in MK and the mixing water on the reaction and properties of MKPGs were investigated.

EXPERIMENTAL

MK, which was obtained by the dehydroxylation reaction of kaolinite, phosphoric acid (PA, 85 %) and distilled water, was used as the raw material. Table 1 lists the chemical compositions of this kaolin as determined by X-ray fluorescence (XRF). Its mineral phases included kaolinite ($Al_2(Si_2O_5)(OH)_4$, PDF#: 80-0885) as the major

phase and quartz (SiO_2, PDF#: 46-1045) as the minor phase (Figure 1). The kaolin was calcined at 750 °C for different lengths of time to obtain the MK. The amount of residual water was calculated using the mass loss of the MK heated to 1000 °C for 1 h (Table 2).

The MK, an appropriate amount of PA, and distilled water were mixed to form geopolymer slurries. A P/Al molar ratio of 1.0 was chosen according to the results of Perera *et al.* [6], Zribi *et al.* [20], and Mathivet *et al.* [16]. The water/MK (W/M) mass ratios were between 0.35 and 0.65. The details of the mixtures are listed in Table 3. The water included the water from the PA, the residual water from the MK, and the additional mixing water. After thorough mixing, the slurry was poured into cylindrical PMMA moulds 30 mm in diameter and 30 mm in height; these specimens were wrapped in plastic film, then cured at 60 °C for 24 h. Thereafter, the hardened mixtures were demoulded and cured for 28 days before testing.

The compressive strength of MKPG samples was measured using an electric servo-motor driven press (HYE-300B, China). The microstructure of the MKPGs was observed by polishing the surfaces of the specimens using a scanning electron microscope (SEM: JEOL JSM-6390A, Japan). The phases were identified by X-ray diffraction (XRD: Bruker D8 Advance, Germany).

Table 1. Chemical composition of the kaolin (mass %).

	SiO$_2$	Al$_2$O$_3$	CaO	Na$_2$O	Fe$_2$O$_3$	K$_2$O	TiO$_2$	Other	LOI*
Kaolin	38.9	35.4	0.2	0.1	0.7	1.2	0.3	3.6	19.6

* Loss on ignition at 1000 °C for 1 h

Table 2. The residual water content in the MK calcined at 750 °C (%).

Time (min)	5	10	15	30	60	300	600
Mass loss (residual water)*	10.5	5.3	4.8	3.6	2.7	2.4	2.2

* Mass loss of the MK calcined at 1000 °C for 1 h after thermal treatment at 750 °C

Table 3. Details of the mixtures of the MKPGs with various W/M ratios.

No.	MK (including residual water) (%)	PA (85 %) (%)	Residual water (%)	Mixing water (%)	W/M ratio	Al/P ratio
Rw1	49.8	44.3	5.23	5.9	0.4	1.0
Rw2	47.0	44.3	2.49	8.7	0.4	1.0
Rw3	46.8	44.3	2.24	8.9	0.4	1.0
Rw4	46.2	44.3	1.66	9.5	0.4	1.0
Rw5/Ew2	45.8	44.3	1.24	9.9	0.4	1.0
Rw6	45.6	44.3	1.09	10.0	0.4	1.0
Rw7	45.5	44.3	1.00	10.2	0.4	1.0
Ew1	46.8	45.3	1.26	7.9	0.35	1.0
Ew2/Rw5	45.8	44.3	1.24	9.9	0.40	1.0
Ew3	44.8	43.4	1.21	10.1	0.45	1.0
Ew4	43.8	42.4	1.18	13.8	0.50	1.0
Ew5	42.9	41.5	1.16	15.5	0.55	1.0
Ew6	42.0	40.6	1.13	17.3	0.60	1.0
Ew7	41.2	39.8	1.11	18.9	0.65	1.0

RESULTS AND DISCUSSION

Phase evolution of kaolin

Figure 1 displays the XRD patterns of the kaolin calcined at 750 °C for different lengths of time. With an increasing calcining time, the diffraction peaks of the kaolinite rapidly become less intense, indicating the progress of the dehydroxylation reaction. After calcination for 30 min, the typical diffraction peaks of kaolinite have disappeared and form a broad diffuse halo from 10° to 20°, centred on 13°, suggesting the transformation of kaolin into an amorphous phase (metakaolinite) [14]. With regards to the calcination from 30 min to 600 min, the resulting MK maintains its amorphous state, however, traces of new diffraction peaks, matching kyanite (Al_2SiO_5, PDF#: 83-1569), are observed in the XRD patterns when the calcination time exceeds 300 min, meaning that the calcining time induces the formation of the ordered structure. Meanwhile, the peaks of quartz remain unchanged during the calcining processes, indicating that calcination at 750 °C cannot induce structural changes in quartz.

From the measured loss of mass from the kaolin (Table 2), 4.8 %, 3.6 %, 2.7 %, 2.4 %, and 2.2 % residual water contents of MK are found after calcining time of 15, 30, 60, 300, and 600 minutes, respectively. The theoretical water in kaolinite is 13.96 %, and the inter-layer water and inner-layer water accounts for two-thirds and one-third of the water, respectively. So, according to the mass loss from the kaolin, 4.8 % residual water is present when it is calcined for 15 min, suggesting that almost all the inter-layer water is lost by dehydroxylation. From the XRD results, the diffraction peaks of kaolinite remain visible in the diffractogram. According to Sperinck *et al.* [13], the kaolinite structure will be completely lost at 80 % dehydroxylation, however, in this MK, 3.6 % residual water is present even as the kaolin is fully transformed to MK as evidenced by the XRD spectra (there is still some water left even after the calcining time beyond that observed by Gasparini *et al.* [14]).

As the MK with different residual water contents is activated by the PA (Rw series), the XRD spectra of the samples change. As shown in Figure 2, regardless of the residual water content, the diffuse halo shifts to 20-35° from 10-20° (2θ values) in the XRD spectra in the Rw series samples, indicating that a geopolymeric reaction has taken place. At a calcining time of 30 min, in which 3.6 % residual water content is found, the typical halo centred at 26° shows the amorphous nature of this MKPG. Also, the peak intensity at *ca.* 26° is increased compared with that in the raw MK material, which is almost the same as that of the quartz phase. This indicates the occurrence of a new phase – berlinite ($AlPO_4$, PDF#: 76-0228) – as proposed in the literature [21]. After a calcining time of 60 min, the intensities of the diffraction spectral peaks are strengthened, indicating an enhanced geopolymerisation reaction. However,

increasing the calcining time leads to a decrease in the amount of $AlPO_4$, indicating that the $AlPO_4$ phase is less completely crystallised. This also evidences the decrease in the reactivity of the MK after a longer calcination time.

As the MK with the different mixing water contents is activated by the PA (Ew series), the colour from the appearance of the MKPG samples lightens from ruby at a W/M ratio of 0.35 to coconut at a W/M ratio of 0.65.
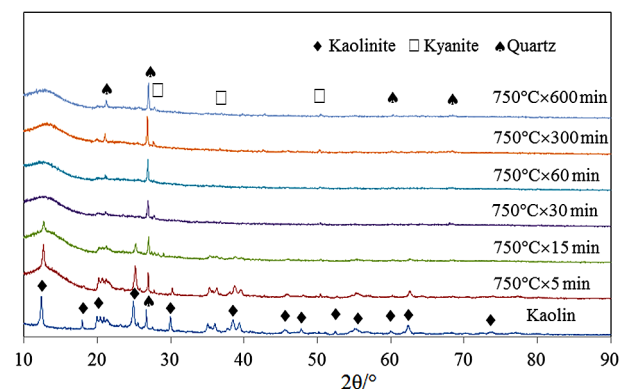

Figure 1. XRD patterns of the kaolin calcined for various lengths of time at 750 °C.
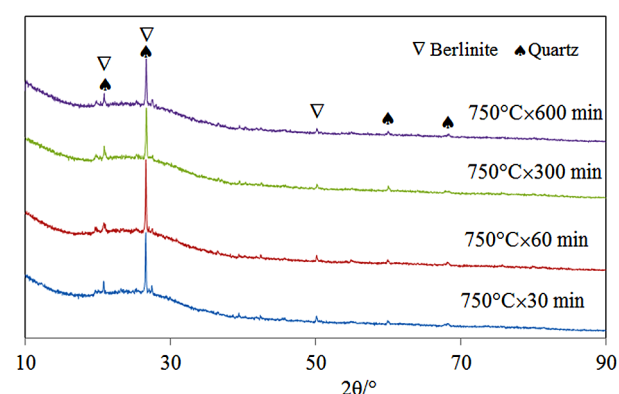

Figure 2. XRD patterns of the MKPGs with kaolin calcined for various lengths of time at 750 °C (the W/M ratio is 0.40).
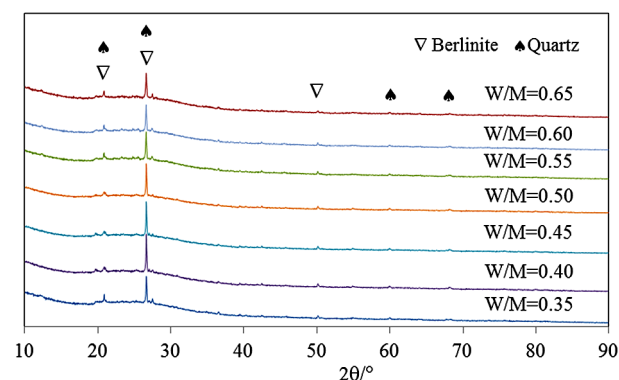

Figure 3. XRD patterns of the MKPGs with various W/M ratios (kaolin calcined at 750 °C for 60 min).

The phase characteristics of the MKPGs with various W/M ratios are also determined by XRD. As shown in Figure 3, the Ew1 to Ew7 samples show similar spectra. The diffuse halo in the XRD spectra, akin to that of the Rw series samples, is observed. This finding also indicated the geopolymeric reaction and amorphous state of the samples in the Ew series. The difference is that the intensity of the $AlPO_4$ phase gradually decreases as the W/M ratio is above 0.40, suggesting the reduced geopolymerisation arises from the additional mixing water.

Compressive strength

The influence of the residual water on the compressive strength of MKPGs is illustrated in Figure 4. When the calcining time is less than 15 min, the MK cannot be activated by the PA due to the high viscosity of the kaolinite, which is not fully transformed to MK, implying that the inter-layer water restrains the geopolymeric processes. At a calcining time of 15 min, the MKPG begins to gain strength. In this case, 4.8 % water is present in the MK and the compressive strength of MKPG is 8.3 MPa. With an increasing calcining time, the compressive strength increases, indicating that the dehydration via removal of the inter-layer water from the kaolin promotes the development of the strength. As only 2.7 % water is contained in the MK (at a calcining time of 60 min), in which, all the inter-layer water has been removed from the MK, a significant increase in the compressive strength occurs. At calcining times of 60 min to 300 min, the compressive strength of the MKPGs varies between 57.6 MPa and 57.3 MPa, demonstrating that some inner-layer water exerts less influence on the development of the geopolymerisation; when the MK is calcined for 600 min, the compressive strength decreases to 43.2 MPa. This indicates that the reactivity of the MK decreases due to the ordered structural formation seen in the XRD spectrum (Figure 1).

From the results above, it can be found that the compressive strength varies in accordance with the changes in the amounts of residual water. In the PA

solution, there are proton H^+ and phosphate groups from the deprotonation, in which, proton H^+ is the impetus for the attack on the MK [22]. If residual water is present, suggesting that an OH^- group exists in the MK, the attacking roles on the MK will be promoted, forming H_2O. However, the residual inter-layer water has a negative influence on the compressive strength; while the inner-layer water exerts less influence on the strength. In fact, the loss of the inter-layer water is related to the structural changes in the kaolinite; but, the loss of the inner-layer water is related to the structural changes of the metakaolinite. When the inter-layer water is lost (representing the formation of an amorphous state), the activation of the MK with the PA will be achieved as found elsewhere [15]. When the inner-layer water begins to be lost, the structure of the MK gradually collapses; however, this does not induce substantial changes in the compressive strength. Only the dehydroxylation of the inner-layer water induces the formation of an ordered state, causing a significant decrease in the compressive strength.

The influence of the mixing water content on the compressive strength is shown in Figure 5. The compressive strength of the MKPG is 38.8 MPa when the W/M ratio is 0.35. With an increase in the W/M ratio, the strength gradually increases. When the W/M ratio is increased to 0.40, the strength of the MKPG reaches 57.6 MPa, which is 32.6 % higher than that of the samples with a W/M ratio of 0.35: however, at higher W/M ratios, the compressive strength decreases, in a manner that is quasi-proportional to the W/M ratio. This trend is in agreement with the literature [18]. As the W/M ratio is increased to 0.65, the compressive strength decreases to 23.0 MPa. Mathivet *et al*. [18] concluded that the water plays two roles in the processes of geopolymerisation: 1) decreasing the viscosity and thus promoting the reaction of the medium; and 2) diluting the concentration of the reactive species and possibly degrading the chemical potential. Therefore, an appropriate amount water is necessary to achieve the most effective geopolymerisation process. In this mixture, the maximum strength of 57.6 MPa is achieved at a W/M ratio of 0.40.
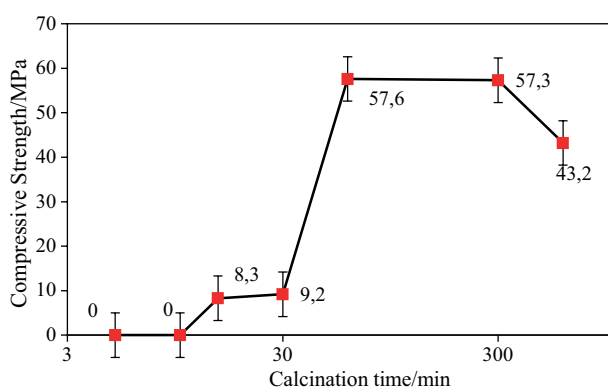

Figure 4. Influence of the calcination time (via the residual water content) on the compressive strength of the MKPGs.
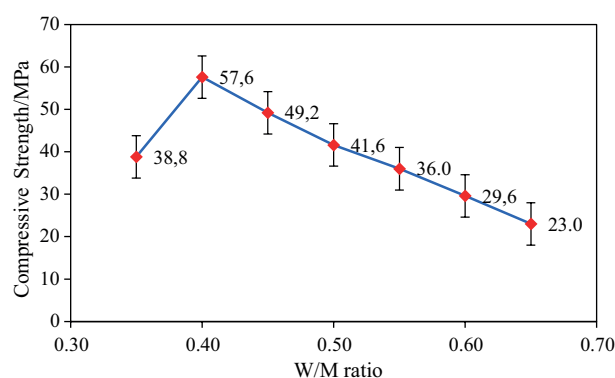

Figure 5. Influence of the W/M ratio (the mixing water content) on the compressive strength of the MKPGs.

Water losses

The further to evaluate the effects of the water on the geopolymerisation process, the water losses of the Ew-series samples were compared at room temperature in a desiccator, at 110 °C, 110 °C to 240 °C, and above 240 °C. As shown in Figure 6, all the samples release water across the various temperature ranges; however, the rates of water losses are obviously different. At room temperature in a desiccator, about 4.3 % of the water is released from sample Ew1, and with increasing W/M ratio, more water is lost. In sample Ew7, in which the W/K ratio is 0.65, about 12.8 % by mass, is released as water.

difference in the water losses narrows to 1.4 % between the samples with the differences in W/M ratios. At 110 °C to 240 °C, the water loss ranges between 1.4-2.1 % with the change in the W/M ratio, and the maximum difference falls to 0.7 %. Above 240 °C, the water losses are less than 1.0 % and vary slightly, regardless of the W/K ratio. The water losses at 110 °C (and beyond) are associated with the physically-absorbed water and the dehydration of the hydrated phases or the chemical-adsorbed water [18, 23].

From the measured water losses, it was found that the losses from the Ew series of the samples have the greatest differences when measured in a desiccator. In comparison, the differences of the losses between the samples are much smaller at 110 °C and above 110 °C. This phenomenon implies that excess water is present in MKPGs as free water rather than as absorbed water leading to the formation of hydrated phases or physically-absorbed phases. The free water loss increases the porosity of the MKPGs, which might be another reason resulting in a decrease in the compressive strength [18]. The physically- or chemically-adsorbed water is almost the same in the Ew-series specimens with the different W/M ratios. During the total mass losses, the loss at 110 °C accounts for a large proportion of the water loss; it appears that most of the water remains as physically-absorbed water in the geopolymers and the water used for the formation of the geopolymer does not participate in the polycondensation reaction to any significant extent [18].
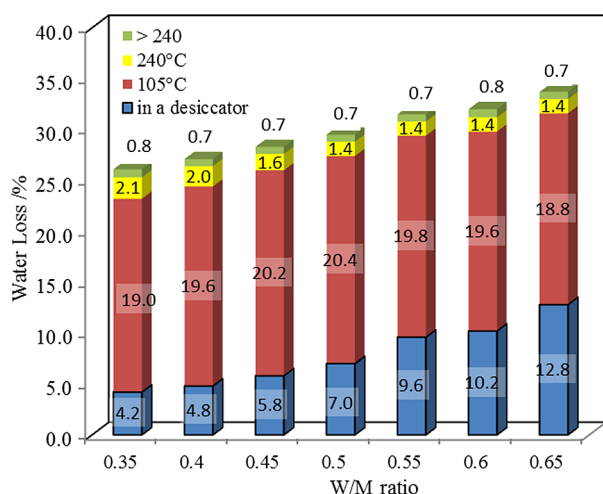

Figure 6. Influence of the W/M ratio (the mixing water) on the mass loss from the MKPGs.

At 110 °C, the rate of loss of the water is higher compared with that in a desiccator, ranging between 19.0-20.4 %, which is much higher than that lost from the specimens in a desiccator; however, the maximum

Microstructural analysis

The morphologies of the MKPGs with the different residual water are shown in Figure 7 (Rw series). The typical plate-like structure of MK can be seen in the sample with 4.8 % residual water (Figures 7a and 7b). This platelet form evidences the presence of unreacted
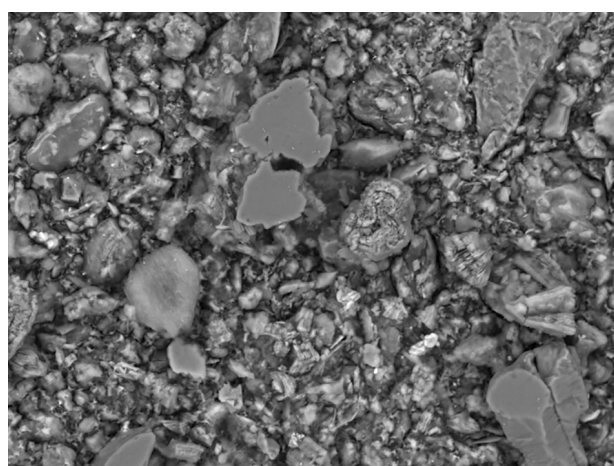
a) Rw3
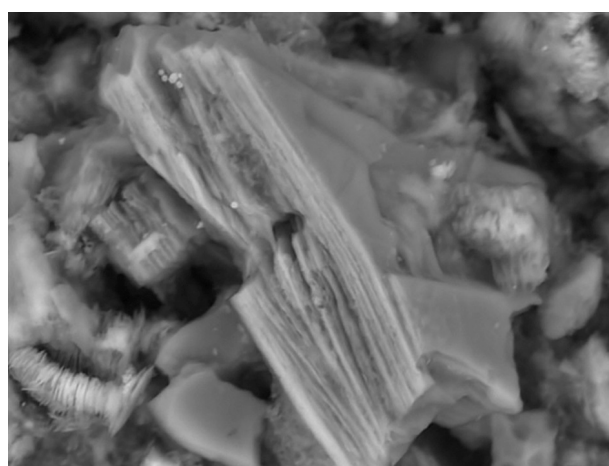
b) Enlarged Rw3

Figure 7. SEM images of the MKPGs of the Rw-series specimens. *(Continue on next page)*

c) Rw5

d) Enlarged Rw5
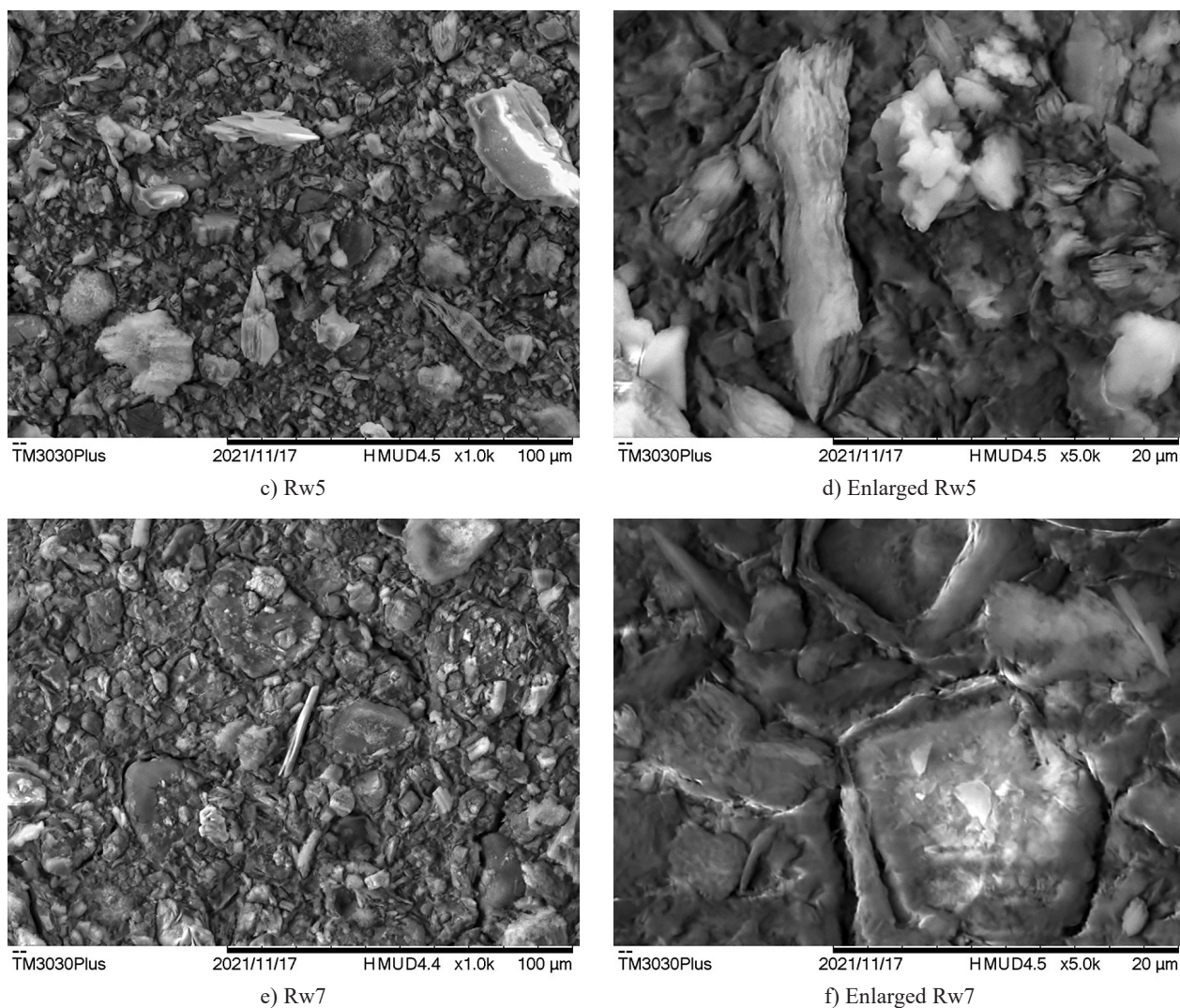

e) Rw7

f) Enlarged Rw7

Figure 7. SEM images of the MKPGs of the Rw-series specimens.

MK [19], which is the cause of the low strength of the MKPGs. With the loss of the residual water, less MK is preserved (Figures 7c and 7d), leading to a greater compressive strength, however, cracks are observed in Rw7 (Figures 7e and 7f) with a further decrease in the residual water content, which induces disorder in terms
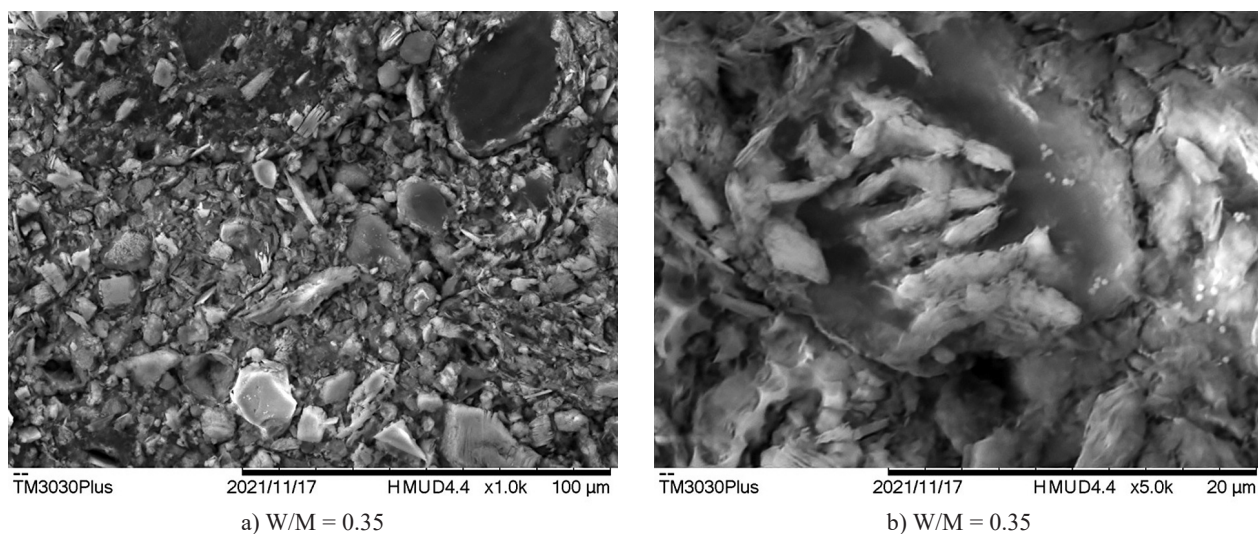

a) W/M = 0.35

b) W/M = 0.35

Figure 8. SEM images of the MKPGs of the Ew-series specimens. *(Continue on next page)*

c) W/M = 0.50

d) W/M = 0.50

e) W/M = 0.55

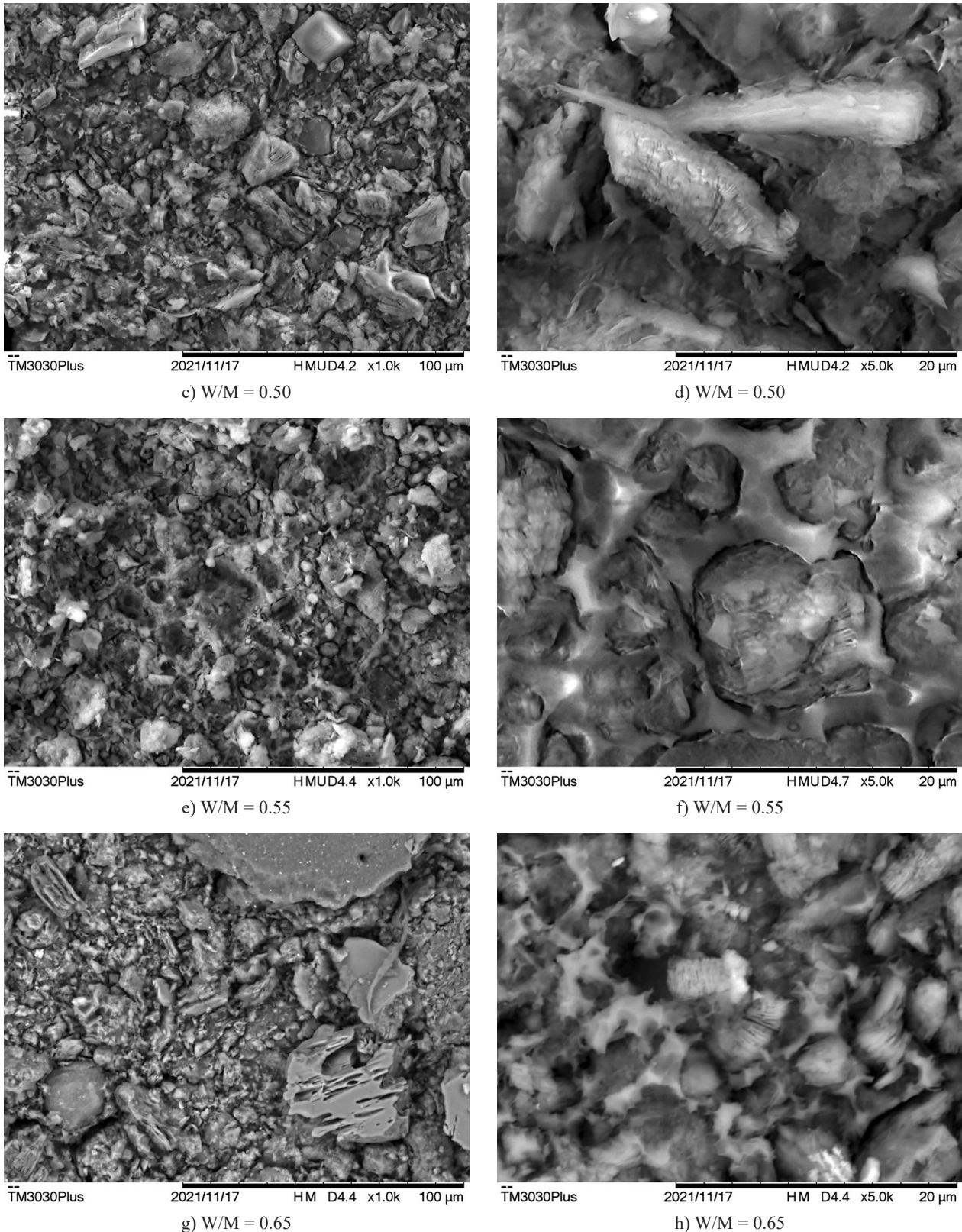f) W/M = 0.55

g) W/M = 0.65

h) W/M = 0.65

Figure 8. SEM images of the MKPGs of the Ew-series specimens.

of the structural formation. From the micrograph of Rw7, large granules are found to be formed, which result in less homogenous, looser microstructures, decreasing the strength of the geopolymer.

At W/M ratios between 0.35 and 0.50, a dense, compacted microstructure is seen on the MKPG surface, indicating an efficient geopolymerisation reaction (Figures 8a-d); however, at W/M ratios above 0.55,

significant changes in the microstructure are observed. Pores and unreacted raw materials are found in the MKPG samples at W/M ratios of 0.55 and 0.65 (Figures 8e-h). Thus, the mixing water in excess that either hinders the geopolymeric processes, or leaves voids due to the volatilisation of water, induces the decreases in the compressive strength. The characteristics of the micrographs in the MKPG samples are in excellent agreement with measured com-pressive strengths (Figure 6).

CONCLUSION

The role of water in an MKPG was investigated. The residual inner-layer water in the MK exerts a negative influence on the compressive strength; the inter-layer water exerts less influence on the strength of the MKPGs. With the increase in the amount of mixing water added, the compressive strength first increases, then decreases in a manner that is quasi-proportional to the W/M ratio. A maximum compressive strength of 57.6 MPa is achieved in the MKPG with the Al/P and W/M ratios of 1.0 and 0.40, respectively. The water-loss testing shows that there is an excess of mixing water present in the MKPGs as free water. The physically-absorbed water and chemically-absorbed water account for 86.8-90.6 % and 9.4-13.2 % of that lost from the hydrated phases, respectively, except for the free water.

REFERENCES

1. Davidovits J. (1994): Geopolymers: Man-made rock geo-synthesis and the resulting development of very early high strength cement. *Journal of Materials Education, 16,* 91-139.
2. Cui X.M., Liu L.P., He Y., Chen J.Y., Zhou, J. (2011): A novel aluminosilicate geopolymer material with low dielectric loss. *Materials Chemistry and Physics,130*, 1-4. Doi: 10.1016/j.matchemphys.2011.06.039
3. Davidovits J. (1991): Geopolymers: inorganic polymeric new materials, *Journal of Thermal Analysis, 37,* 1633-1656. Doi: 10.1007/BF01912193
4. Zribi M., Samet B., Baklouti S. (2019): Effect of curing temperature on the synthesis, structure and mechanical properties of phosphate-based geopolymers. *Journal of Non-Crystalline Solids, 511,* 62-67. Doi: 10.1016/j.jnoncrysol.2019.01.032
5. Cao D.G., Su D.G., Lu B., Yang Y.X. (2005): Synthesis and structure characterization of geopolymeric material based on metakaolinite phosphoric acid. *Journal of the Chinese Ceramic Society*, *33*, 1385-1389. Doi: 10.3321/j.issn:0454-5648.2005.11.018
6. Perera D.S., Hanna J.V., Davis J., Blackford M.G., Latella B.A., Sasaki Y., Vance E.R. (2008): Relative strengths of phosphoric acid-reacted and alkali-reacted metakaolin materials. *Journal of Materials Science, 43*, 6562-6566. Doi: 10.1007/s10853-008-2913-6
7. Wagh A.S. (2004): Chemical bonded phosphate ceramic
   – a novel class of geopolymers, In: Proceedings of the 106th Annual Meeting of The American Ceramic Society, *Advances in Ceramic Matrix Composites X.* Indianapolis, pp. 107-116.
8. Douiri H., Louati S., Baklouti S., Arous M., Fakhfakh Z. (2016): Enhanced dielectric performance of metakaolin-H_3PO_4 geopolymers. *Materials Letters*, *164*, 299-302. Doi: 10.1016/j.matlet.2015.10.172
9. Liu L.P., Cui X.M., He Y., Liu S.D., Gong S.Y. (2012): The phase evolution of phosphoric acid-based geopolymers at elevated temperatures. *Materials Letters*, *66,* 10-12. Doi: 10.1016/j.matlet.2011.08.043
10. Douiri H., Louati S., Baklouti S., Arous M., Fakhfakh Z. (2014): Structural, thermal and dielectric properties of phosphoric acid-based geopolymers with different amounts of H_3PO_4. *Materials Letters, 116*, 9-12. Doi: 10.1016/j.matlet.2013.10.075
11. Lin H., Liu H., Li Y., Kong X. (2021): Properties and reaction mechanism of phosphoric acid activated metakaolin geopolymer at varied curing temperatures, *Cement and Concrete Research*, *144*,106425. Doi: 10.1016/j.cemconres.2021.106425
12. Louati S., Hajjaji W., Baklouti S., Samet B. (2014): Structure and properties of new eco-material obtained by phosphoric acid attack of natural Tunisian clay. *Applied Clay Science*, *101*, 60-67. Doi: 10.1016/j.clay.2014.07.015
13. Sperinck S., Raiteri P., Marks N., Wright K. (2011): Dehydroxylation of kaolinite to metakaolin – a molecular dynamics study. *Journal of Materials Chemistry*, *21*, 2118-2125. Doi: 10.1039/C0JM01748E
14. Gasparini E., Tarantino S.C., Ghigna P., Riccardi M.P., Cedillo-González E.I., Siligardi C., Zema M. (2013): Thermal dehydroxylation of kaolinite under isothermal conditions. *Applied Clay Science*, *80-81*,417-425. Doi: 10.1016/j.clay.2013.07.017
15. Cao D.G., Su D.G., Yang Z.Y., Song G.S. (2004): Study of the microstructure of metakaolinite with IR, TG, SEM, XRD methods. *Acta Mineralogica Sinica*, *24,* 366-372. Doi: 10.3321/j.issn:1000-4734.2004.04.009
16. Mathivet V., Jouin J., Gharzouni A., Sobrados I., Celerier H., Rossignol S., Parlier M. (2019): Acid-based geopolymers: understanding of the structural evolutions during consolidation and after thermal treatments. *Journal of Non-Crystalline Solids, 512*,90-97. Doi: 10.1016/j.jnoncrysol.2019.02.025
17. Tchakouté H.K., Rüscher C.H., Kamseu E., Djobo J.N.Y., Leonelli C. (2017): The influence of gibbsite in kaolin and the formation of berlinite on the properties of metakaolin-phosphate-based geopolymer cements. *Materials Chemistry and Physics,199*, 280-288. Doi: 10.1016/j.matchemphys.2017.07.020
18. Mathivet V., Jouin J., Parlier M., Rossignol S. (2021): Control of the alumino-silico-phosphate geopolymers properties and structure by the phosphorus concentration. *Materials Chemistry and Physics*,*258*,123867. Doi: 10.1016/j.matchemphys.2020.123867
19. Derouiche R., Baklouti S. (2021): Phosphoric acid based geopolymerisation: Effect of the mechanochemical and the thermal activation of the kaolin. *Ceramics International*, *47*,13446-13456. Doi: 10.1016/j.ceramint.2021.01.203
20. Zribi M., Samet B., Baklouti S. (2020): Mechanical, microstructural and structural investigation of phosphate-based geopolymers with respect to P/Al molar ratio. *Journal of*

Solid State Chemistry, *281*,121025. Doi: 10.1016/j.jssc. 2019.121025

21. Gualtieri M.L., Romagnoli M., Gualtieri A.F. (2015): Preparation of phosphoric acid-based geopolymer foams using limestone as pore forming agent-Thermal properties by in situ XRPD and Rietveld refinements. *Journal of the European Ceramic Society*, *35*, 3167-3178. Doi: 10.1016/j. jeurceramsoc.2015.04.030

22. Tchakouté H.K., Rüscher C.H., Kamseu E., Andreola F., Leonelli C. (2017): Influence of the molar concentration of phosphoric acid solution on the properties of metakaolin-phosphate-based geopolymer cements. *Applied Clay Science*, *147*,184-194. Doi: 10.1016/j.clay.2017.07.036

23. Celerier H., Jouin J., Mathivet V., Tessier-Doyen N., Rossignol S. (2018): Composition and properties of phosphoric acid-based geopolymers, *Journal of Non-Crystalline Solids*, *493*,94-98. Doi: 10.1016/j.jnoncrysol.2018.04.044